Dalton Transactions

PAPER

View Article Online
View Journal | View Issue

Cite this: *Dalton Trans.*, 2015, **44**, 3544

DNA fragment conformations in adducts with Kiteplatin†

Nicola Margiotta,*[a] Emanuele Petruzzella,[a] James A. Platts,[b] Shaun T. Mutter,[b] Robert J. Deeth,[c] Rosa Ranaldo,[a,d] Paride Papadia,[e] Patricia A. Marzilli,[d] Luigi G. Marzilli,[d] James D. Hoeschele[f] and Giovanni Natile*[a]

The anticancer activity of cisplatin is triggered by its formation of intrastrand adducts involving adjacent G residues of DNA. To obtain information on the different conformers that can be formed, carrier ligands such as 2,2′-bipiperidine, which provide large steric bulk near the platinum coordination plane and decrease the dynamic motion about the Pt–N7 bonds, were introduced ("retro-modelling" approach). In the present study we investigate the effect of *cis*-1,4-diaminocyclohexane (*cis*-1,4-DACH) on the formation, stability, and stereochemistry of (*cis*-1,4-DACH)Pt(ss-oligo) adducts (ss-oligo = d(GpG) with 3′- and/or 5′-substituents). Interesting features of this ligand, absent in previous retro-modelling studies, include the large bite angle (expected to impede the ease of interconversion between possible conformers), the presence of two protons on each nitrogen (a characteristic associated with antitumor activity), and the absence of chiral centres. The use of *cis*-1,4-DACH has made it possible to detect different conformers in a system containing a primary diamine carrier ligand associated with anticancer activity and to confirm the previous hypothesis that the coexistence of different conformers established in studies of retro models having relatively bulky ligands is not an artefact resulting from carrier-ligand bulk. Moreover, the data for the (*cis*-1,4-DACH)Pt(d(GpG)) and (*cis*-1,4-DACH)Pt(d(GGTTT)) adducts indicate that at a temperature close to the physiological one (40 °C) HH1 and ΔHT1 conformers are present in comparable amounts. In contrast, at low temperature (close to 0 °C) the equilibrium shifts dramatically toward the more stable HH1 conformer (for the (*cis*-1,4-DACH)Pt(d(TGGT)) adduct the HH1 conformer is always dominant, even at high temperature). Notably, (*cis*-1,4-DACH)$PtCl_2$ (Kiteplatin) has been recently reinvestigated and found to be particularly active against colorectal cancer (including oxaliplatin-resistant phenotypes).

Received 16th June 2014,
Accepted 6th August 2014

DOI: 10.1039/c4dt01796j

www.rsc.org/dalton

Introduction

The anticancer activity of cisplatin, *cis*-[$PtCl_2(NH_3)_2$], the prototype of platinum-based anticancer-drugs, is triggered by the formation of intrastrand adducts involving Pt binding to the N7 of two adjacent G residues of DNA.[1–3] The two cross-linked guanine bases adopt primarily a head-to-head (HH) arrangement (Fig. 1), with both G residues maintaining the *anti* conformation typical of B-DNA (HH1 in Fig. 1).[2,4–10] In contrast, in interstrand cross-links, the guanine bases from the two strands adopt a head-to-tail (HT) arrangement.[11–14] Such interstrand cross-links could also contribute to the anticancer activity.[15,16]

All evidence indicates that the HH1 conformer is clearly dominant in cisplatin-(~GpG~) intrastrand adducts in which a platinated strand is in a DNA duplex.[11,17–26] However, in the simple *cis*-$(NH_3)_2$Pt(d(GpG)) model and in *cis*-$(NH_3)_2$Pt(ss-oligo) models (oligo = oligodeoxyribonucleotide, ss = single strand), the dynamic nature of these adducts complicates the

[a]*Dipartimento di Chimica, Università degli Studi di Bari A. Moro, via E. Orabona, 4, 70125 Bari, Italy. E-mail: nicola.margiotta@uniba.it, giovanni.natile@uniba.it; Tel: +39 080 5442759; +39 080 5442774*
[b]*School of Chemistry, Cardiff University, Park Place, Cardiff, CF10 3AT, UK*
[c]*Department of Chemistry, University of Warwick, Gibbet Hill Road, Coventry, CV4 7AL, UK*
[d]*Department of Chemistry, Louisiana State University, Baton Rouge, Louisiana 70803, USA*
[e]*Dipartimento di Scienze e Tecnologie Biologiche ed Ambientali, Università del Salento, Prov.le Lecce-Monteroni, 73100 Lecce, Italy*
[f]*Department of Chemistry, Eastern Michigan University, Ypsilanti, Michigan 48197, USA*

†Electronic supplementary information (ESI) available: Tables S1 and S2: ^{1}H and ^{31}P NMR data at different temperatures of (*cis*-1,4-DACH)Pt(d(TGGT)). Fig. S1: Formation of (*cis*-1,4-DACH)Pt(d(GPG)) monitored by ^{1}H NMR. Fig. S2 and S3: Formation of (*cis*-1,4-DACH)Pt(d(GGTTT)) monitored by ^{1}H and ^{31}P NMR, respectively. Fig. S4: Formation of (*cis*-1,4-DACH)Pt(d(TGGT)) monitored by ^{1}H NMR. Fig. S5: Structure of d(TGGT) with proton numbering. Fig. S6: ^{31}P NMR of (*cis*-1,4-DACH)Pt(d(TGGT)). Fig. S7: ^{31}P NMR of (*cis*-1,4-DACH)Pt-(d(TGGT)) at different temperatures. Fig. S8: Temperature dependence of H1′ signals of (*cis*-1,4-DACH)Pt(d(TGGT)). See DOI: 10.1039/c4dt01796j

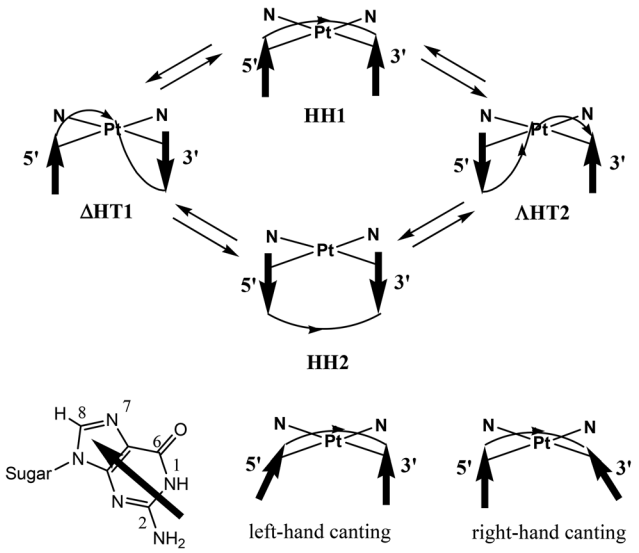

Fig. 1 Possible conformers of *cis*-A_2Pt(∼GpG∼) cross-links (A_2 = two amines or a bidentate diamine; (∼GpG∼) = adjacent G residues in oligodeoxyribonucleotides). The arrows represent the G bases, and the phosphodiester backbone (placed in the front) is represented by a curved line linking the two arrows. Interconversion between conformers is possible *via* rotation about the Pt–G bonds. HT1 and HT2 differ, respectively, for the Δ and Λ handedness of the two straight lines, one perpendicular to the coordination plane and passing through Pt and the other connecting the O6 atoms of the two guanines. HH1 and HH2 differ, respectively, for the north or south orientations of the arrows representing the guanines, having placed 5′-G on the left- and 3′-G on the right-hand side. Canting handedness is defined by two straight lines, one connecting the N7 atoms of the two coordinated guanines and the other overlapping the arrow representing a given guanine.

NMR spectroscopic analysis. In the limiting case in which rotation about the Pt–N7 bonds is fast on the NMR time scale, the informative potential of the NMR technique cannot be realized.[4–6,27–44] Watson–Crick base pairing reduces conformational dynamics in duplexes.[17–26]

In cases in which the intrastrand cross-link clearly has an HH1 conformation, such as in *cis*-A_2Pt(d-oligo) adducts (d-oligo = duplexed oligodeoxyribonucleotides; A_2 = two monodentate or one bidentate N donor carrier ligand), the H8 signals of the two Gs are not well separated ($\delta \sim 0.3$ ppm), with the 3′-G H8 upfield and the 5′-G H8 downfield. The 3′-G base is canted, and the 3′-G H8 is positioned near the anisotropic region of the 5′-G base.[20,21,23,26,45] This is called right-handed (R) canting because the straight line connecting the N7 of the two coordinated guanines and the arrow mimicking the 3′-G base can be represented by the index and thumb of the right hand (Fig. 1). In *cis*-A_2Pt(ss-oligo) adducts in which A_2 is a non-bulky ligand, the 5′-G H8 is positioned by 5′-G base canting near the anisotropic 3′-G base. Such left-handed (L) canted adducts (the straight line connecting the N7 of the two coordinated guanines and the arrow mimicking the 5′-G base are represented by the index and thumb of the left hand, Fig. 1) have an upfield 5′-G H8 signal and a very downfield 3′-G H8 signal. This signal separation is clear and large when the cross-link is not at the 5′ end of the ss-oligo,[5,6,27,31,33,34,43] *i.e.*, when there is at least one nucleotide residue in the position 5′ to the 5′-G in the cross-link.

To obtain information on the different conformers, many investigators have studied adducts of short ss-oligos by employing the Marzilli and Natile "retro-modelling" approach.[17,46–53] These studies used carrier ligands (A_2) that provide large steric bulk in or near the platinum coordination plane in order to decrease the dynamic motion about the Pt–N7 bonds, thus allowing multiple conformers to coexist and to interconvert slowly on the NMR time scale, even if the adducts involved ss-oligos.[11,17,46–48,54–57] Studies of retro models have shown that all major conformers (namely, HH1, HH2, ΔHT1, and ΛHT2, Fig. 1) are possible.[17,46,58–63] These major conformers, in turn, can have several sub-forms differing in backbone conformation and base canting (R or L).

One of the most successful carrier ligands used in retro models has been 2,2′-bipiperidine (Bip) (Chart 1) in two different configurations (*S*,*R*,*R*,*S* or *R*,*S*,*S*,*R* configurations at the N, C, C, and N chelate ring atoms).[17,46–48,53,55,59,64] The stereochemistry of the Bip carrier ligand influences both the conformer distribution and the cross-link handedness. For example, ((*R*,*S*,*S*,*R*)-Bip)Pt(d(GpG)) was shown to have two abundant right-handed conformers (HH1 R, HH2 R), and ((*S*,*R*,*R*,*S*)-Bip)Pt(d(GpG)) was shown to have two abundant left-handed conformers (HH1 L, ΔHT1 L).[17,46,59] In these conformers at least one guanine base is oriented such that its O6 is on the same side of the coordination plane as a Bip NH proton; thus, a G O6-NH hydrogen bond could form. In each case, the observed base canting direction of that G residue permits such H-bonding. Another successful ligand in "retro-model" studies was the *N*,*N*,*N*′,*N*′-tetramethyl-2,3-diaminobutane ligand (Me_4DAB), with *S*,*S* or *R*,*R* configurations at the chelate ring atoms (Chart 1), and showing analogous results.[10,58]

Our objective in the present study was to assess the properties of *cis*-1,4-diaminocyclohexane (*cis*-1,4-DACH) by determining the effect of the carrier ligand on the formation, stability, and stereochemistry of (*cis*-1,4-DACH)Pt(ss-oligo) adducts. An interesting feature of this ligand is its ∼97° bite angle,[65] which is larger than that of cisplatin (∼90°; Chart 2)

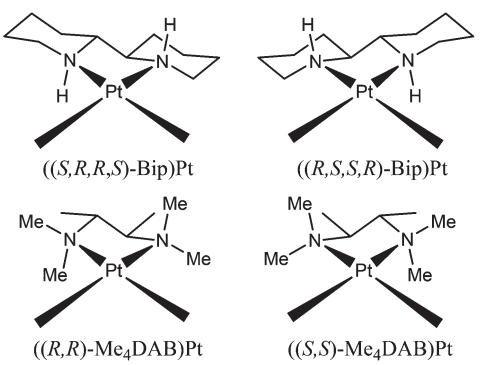

Chart 1

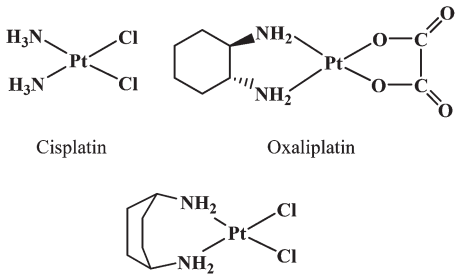

Chart 2

and of analogous compounds with ethylenediamine (en, 83°)[66] or 1,2-DACH (83.2°, average value of three Pt complexes).[67] The large bite angle of *cis*-1,4-DACH complexes could also reduce the (amine)NH_2–Pt–N7(G) angles, thus possibly influencing the distribution of conformers and likely diminishing the ease of interconversion between possible conformers. Such an impeded interconversion was reported for the (*cis*-1,4-DACH)Pt-(5′-GMP)$_2$ adduct (having two untethered guanine derivatives), for which ^{1}H NMR evidence for all three possible conformers (HH, ΔHT, and ΛHT) was observed by lowering the temperature to −35 °C. (For such adducts with untethered guanine bases, conformer designations lack the 1 and 2, which designate backbone direction, and the HH1 and HH2 conformers shown in Fig. 1 become equivalent.)[65] The equilibrium composition of the three conformers was 33% HH, 51% ΛHT, and 16% ΔHT. The high abundance of the ΛHT conformer arises from "second-sphere communication" in which the 5′-phosphate of each 5′-GMP interacts with the guanine base NH group of the *cis*-5′-GMP.[10] Another key feature of the *cis*-1,4-DACH ligand is that both donors are primary amines. This characteristic, which was not explored in previous retro-model studies, usually favours antitumour activity. Finally, the 1*R*,2*R*-DACH ligand in the anticancer drug oxaliplatin ((1*R*,2*R*-DACH)-Pt(oxalate), Chart 2) and amine ligands used in retro-model studies have chiral centres, while *cis*-1,4-DACH has no chiral centres and hence cannot influence the chirality of (*cis*-1,4-DACH)Pt(DNA) adducts.

The *cis*-1,4-DACH carrier ligand was introduced into platinum-based drug research many years ago, as an alternative to 1*R*,2*R*-DACH in oxaliplatin, a third generation platinum drug with a spectrum of activity not superimposable on that of cisplatin.[68] However, after some initial interest, *cis*-1,4-DACH was set aside. More recently, [$PtCl_2$(*cis*-1,4-DACH)] (Kiteplatin, Chart 2) was extensively reinvestigated by some of us, and it was found to have potential application against colorectal cancer (including oxaliplatin-resistant phenotypes).[65,69–73]

In this work, (*cis*-1,4-DACH)Pt(d(GpG)), (*cis*-1,4-DACH)Pt-(d(GGTTT)), and (*cis*-1,4-DACH)Pt(d(TGGT)) adducts were investigated by employing ^{1}H and ^{31}P NMR spectroscopy complemented with a combination of molecular mechanics and semi-empirical quantum-chemical calculations. It should be noted that the triplet GGT present in the latter two adducts is also part of the repetitive sequence in single-strand telomeres, which could also be potential targets for platinum drugs.[63,74–76]

Experimental section

Materials and methods

NMR spectra were recorded on Bruker instruments (Avance DPX 300 MHz, Avance DPX 400 MHz, Avance II 600 MHz, and Avance III 700 MHz) equipped with variable-temperature units. Standard Bruker pulse sequences were employed for the NMR experiments, using gradient selected versions when necessary. In particular, 2D NMR spectra (NOESY, COSY, TOCSY) with water suppression were obtained by using the standard Bruker sequence with presaturation or excitation sculpting.[77]

DNO_3 and NaOD solutions (0.1 M in D_2O) were used to adjust the pH of the D_2O solutions. ^{1}H NMR experiments at different temperatures were referenced to the residual HOD peak (^{1}H). ^{1}H-decoupled ^{31}P NMR spectra were recorded using trimethyl phosphate (TMP) in D_2O as an external reference (+2.10 ppm with respect to H_3PO_4, 85% m/m, placed at 0 ppm). The spectra recorded at −10 °C, on samples dissolved in D_2O–CD_3OD (70/30, v/v), were referenced to the internal residual peak of CD_3OD (^{1}H) or external TMP (^{31}P) dissolved in the same mixture.

Deoxyguanyl(3′–5′)deoxyguanosine (d(GpG)) was purchased from Sigma and was, in part, also provided by Prof. Jan Reedijk (Leiden University, The Netherlands). d(GGTTT) and d(TGGT) were synthesized at the Emory Microchemistry Facility (Atlanta, GA) and purified by FPLC, using deionized water and 2 M NaCl water solution as eluents. Oligonucleotide concentrations were determined by using the following ε_{260} at 25 °C: 46 300 M^{-1} cm^{-1} for d(GGTTT) and 37 600 M^{-1} cm^{-1} for d(TGGT).[78]

The *cis*-1,4-DACH carrier ligand and the [$PtCl_2$(*cis*-1,4-DACH)] complex were synthesized according to previously described procedures.[65,79–81] As is commonly done, we used an activated form of the platinum dichlorido drug, [$Pt(OSO_3)$-(OH_2)(*cis*-1,4-DACH)], to produce the reactive diaqua species after equilibration in water. [$Pt(OSO_3)(OH_2)$(*cis*-1,4-DACH)] was prepared from [$PtCl_2$(*cis*-1,4-DACH)] (60 mg, 0.16 mmol), suspended in water (15 mL), and treated with Ag_2SO_4 (49.9 mg, 0.16 mmol). After stirring for 24 h at room temperature, the suspension was filtered through Celite to remove AgCl and the solvent evaporated to dryness under reduced pressure. The white residue was the desired product (yield, 56.9 mg, 0.13 mmol, 81%). Anal. calculated for [$Pt(OSO_3)(OH_2)$(*cis*-1,4-DACH)]·H_2O ($C_6H_{18}N_2O_6SPt$): C, 16.33; H, 4.11; N, 6.35%. Found: C, 16.50; H, 4.04; N, 6.33%.

Preparation of samples for NMR investigation

(*cis*-1,4-DACH)Pt(d(GpG)) was prepared from [$Pt(OSO_3)(OH_2)$-(*cis*-1,4-DACH)] (1.2 mg, 0.0028 mmol) dissolved in D_2O (0.55 mL), left equilibrating at room temperature for 4 days and then treated with d(GpG) (1.91 mg, 0.031 mmol;

Pt : d(GpG) ratio of 1 : 1.1). The pH of the solution was adjusted to ~3 with DNO_3 and the sample was kept at 5 °C. The progress of the reaction was monitored by ^{1}H NMR spectroscopy, and the disappearance of the G H8 signals of free d(GpG) indicated that the reaction was complete.

(*cis*-1,4-DACH)Pt(d(GGTTT)) was prepared similarly to the previous adduct from [Pt(OSO$_3$)(OH$_2$)(*cis*-1,4-DACH)] (1.17 mg, 0.0027 mmol), dissolved in D_2O (0.690 mL), and, after equilibration for 4 days at room temperature, treated with d(GGTTT) (4.1 mg, 0.0027 mmol; 1 : 1.1 Pt : d(GGTTT) ratio). The reaction progress (room temperature) was monitored by ^{1}H NMR spectroscopy using the G H8 and the T H6 signals of free d(GGTTT) as indicators; the pH was always ~4.

(*cis*-1,4-DACH)Pt(d(TGGT)) was also prepared in a similar way from [Pt(OSO$_3$)(OH$_2$)(*cis*-1,4-DACH)] (1.23 mg, 0.0029 mmol) dissolved in D_2O (0.690 mL), left to equilibrate at room temperature for 4 days, and then treated with d(TGGT) (3.49 mg, 0.0029 mmol; 1 : 1.1 Pt : d(TGGT) ratio). The reaction progress (room temperature) was monitored by ^{1}H NMR spectroscopy by using the G H8 and the T H6 signals of free d(TGGT) as indicators; the pH was always ~4.

Calculations

A DNA adduct was constructed from PDB entry 1PGC through truncation to two coordinated guanines plus the backbone, and 1,2-DACH was converted into its 1,4 isomer manually, retaining the position of the Pt and N atoms and adapting cyclohexane into a boat-like conformation. Semi-empirical calculations employed MOPAC with the PM6-DH2 method.[82–84] Conformational freedom was explored by stochastic conformational searching of all rotatable bonds in the d(GpG) adduct using Deeth's ligand field molecular mechanics (LFMM) approach[85] with previously reported parameters for Pt(II)[86,87] and with AMBER99 parameters for all other atoms[88] and incorporating the Born model of aqueous solvation as implemented in the DommiMOE[89] extension to MOE.[90]

Results and discussion

Reaction with d(GpG)

A solution of the activated form of Kiteplatin, [Pt(OD$_2$)$_2$(*cis*-1,4-DACH)]$^{2+}$, and d(GpG) (1 : 1.1 molar ratio, 5 mM concentration in D_2O) at 5 °C and pH ~ 3, prepared as above, was monitored over time by ^{1}H NMR spectroscopy (Fig. S1 in the ESI†). Within a few days, the H8 signals of free d(GpG) (8.14 and 7.95 ppm for 3′-G and 5′-G, respectively) completely disappeared, accompanied by the appearance of new, very broad downfield-shifted H8 signals; this shift is consistent with formation of (*cis*-1,4-DACH)Pt(d(GpG)) adducts. The G H1′ signals, which in free d(GpG) fall at 6.22 (3′-G) and 6.07 ppm (5′-G), merged into a broad feature centred at 6.22 ppm upon platination (Fig. S1†). The methynic and methylenic signals of *cis*-1,4-DACH (respectively at 3.23 and 1.77 ppm in [Pt(OD$_2$)$_2$(*cis*-1,4-DACH)]$^{2+}$) shifted downfield (to 3.40 and 1.89 ppm) upon reaction with d(GpG).

Temperature effect. The broadness of the H8 signals indicates that more conformers of the (*cis*-1,4-DACH)Pt(d(GpG)) adduct are present in D_2O solution at 25 °C and that the conformers interconvert at a rate which is comparable to the NMR time scale. A previous study showed that, by lowering the temperature to −35 °C (solvent D_2O–CD_3OD, 2 : 1, v/v), it was possible to identify different conformers of the (*cis*-1,4-DACH)-Pt(5′-GMP)$_2$ adduct with untethered guanines.[65] Therefore, in the present study we used a (*cis*-1,4-DACH)Pt(d(GpG)) sample in D_2O–CD_3OD (2 : 1, v/v) to record NMR spectra at different temperatures (Fig. 2). As the temperature was raised, the broad H8 signals in the 8.40–8.00 ppm region became sharper, and at 55 °C the sample showed two major, rather sharp, H8 signals at 8.41 and 8.18 ppm, but there were still some broad H8 signals, indicating that in addition to the major (*cis*-1,4-DACH)Pt(d(GpG)) monomeric adduct, other species (possibly platinum oligomers) were also present. Upon cooling to 25 °C, the NMR sample had the same spectrum as before heating. This reversible, temperature-dependent spectral change confirms that at room temperature the major component of the sample is an adduct consisting of two or more conformers that interconvert at a rate comparable to the NMR time scale.

Lowering the temperature of the NMR sample caused decoalescence of the broad H8 NMR signal observed at 25 °C and, at the lowest temperature reached in the experiment (−10 °C), two sharp H8 signals of equal intensity (at 8.94 and 8.46 ppm, Fig. 2) were observed, together with a more shielded, very broad, H8 feature. Warming the NMR sample

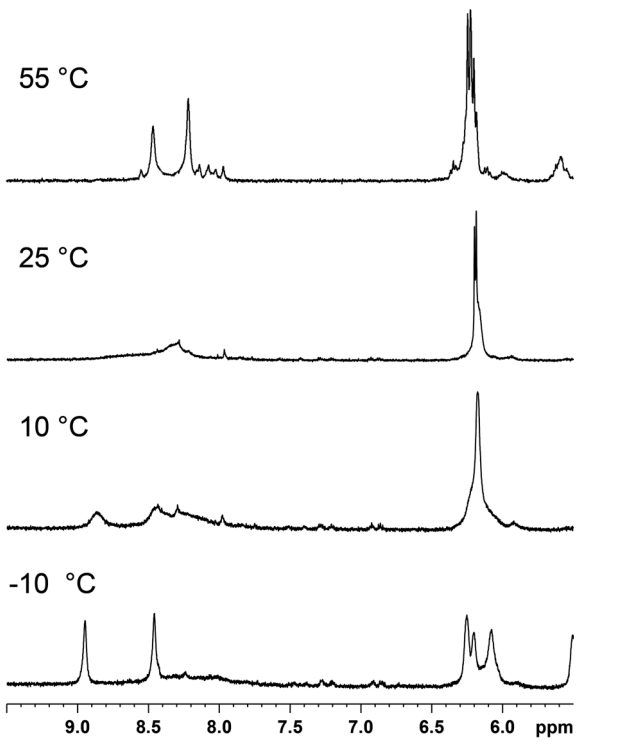

Fig. 2 ^{1}H NMR (600 MHz) spectra in the region of H8 and H1′ resonances for the (*cis*-1,4-DACH)Pt(d(GpG)) adduct in D_2O–CD_3OD (2 : 1, v/v) at different temperatures.

back to room temperature restored the initial spectrum, confirming the presence of a dynamic equilibrium.

In order to assign the two sharp H8 peaks of equal intensity detected at −10 °C to the corresponding conformer of (*cis*-1,4-DACH)Pt(d(GpG)), we used a combination of 1D and 2D NMR methods (NOESY, DQF-COSY, TOCSY, [^{1}H,^{13}C] HSQC, and ^{31}P NMR). The 2D NOESY spectrum at −10 °C (Fig. 3) showed an NOE cross-peak between the two sharp H8 signals (8.94 and 8.46 ppm). An H8–H8 cross-peak is indicative of an HH conformer.[10,11,24] The more upfield H8 signal (8.46 ppm) showed two strong NOE cross-peaks to signals at 2.45 and 2.78 ppm. An NOE cross-peak was also observed between the 2.45 and 2.78 ppm signals. Moreover, both signals showed a cross-peak to a signal at 6.08 ppm. The latter signal at 6.08 ppm had another NOE cross-peak to a signal at 4.08 ppm. The H8 signal at 8.46 ppm also showed a strong NOE cross-peak to a signal at 5.00 ppm. All these data, along with TOCSY data, allowed us to assign the signals at 6.08, 2.45, 2.78, 5.00, and 4.08 ppm to H1′, H2′, H2″, H3′, and H4′ sugar protons, respectively (Table 1). The strong H8–H3′ NOE cross-peak indicates an N-sugar pucker,[46,91,92] a characteristic of a 5′-G residue.[46] Strong H8–H2′ and H8–H2″ NOE cross-peaks and an almost undetectable H8–H1′ NOE cross-peak are all consistent with the 5′-G residue having an *anti* conformation.[59]

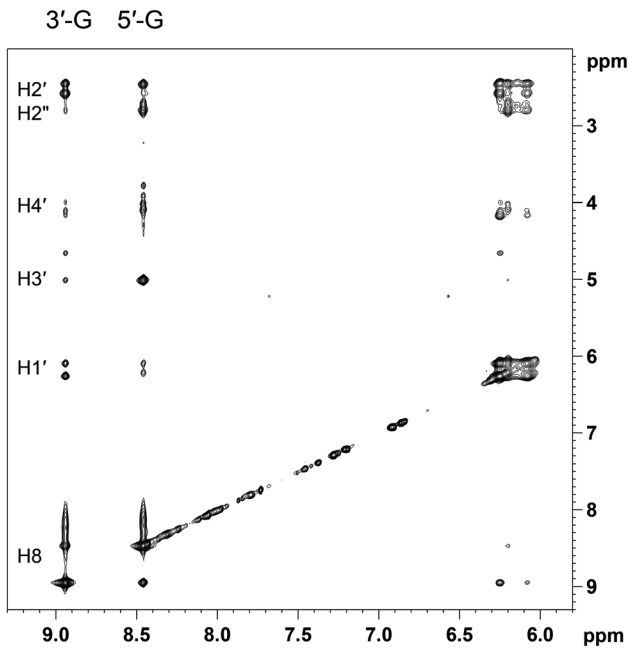

Fig. 3 Selected region of the 2D NOESY (600 MHz) spectrum obtained for (*cis*-1,4-DACH)Pt(d(GpG)) in D_2O–CD_3OD (2 : 1, v/v) at −10 °C.

The more downfield H8 signal (8.94 ppm) showed strong NOE cross-peaks to signals at 2.45 and 2.57 ppm. The latter two signals are connected by an NOE cross-peak. In addition, both signals at 2.45 and 2.57 ppm have comparably intense NOE cross-peaks to a signal at 6.26 ppm. An additional NOE cross-peak is observed between signals at 6.26 and 4.16 ppm. The latter has a cross-peak with a signal at 4.64 ppm. These observations, along with TOCSY data, allow assignment of the signals at 6.26, 2.45, 2.57, 4.64, and 4.16 ppm to the H1′, H2′, H2″, H3′, and H4′ sugar protons, respectively (Table 1). The absence of a significant H8–H3′ NOE cross-peak suggests that the sugar of this residue retains the S pucker, a characteristic of a 3′-G residue;[91] thus, the downfield H8 signal belongs to the 3′-G residue. The strong intranucleotide 3′-G H8–H2′/H2″ NOE cross-peaks and the weak 3′-G H8–H1′ NOE cross-peak indicate that the 3′-G residue has *anti* conformation.[91] The combination of two *anti* G residues and downfield 3′-G H8 and upfield 5′-G H8 signals is a clear indication of left-hand canting of the 5′-G residue, a common feature of *cis*-A_2Pt(ss-oligo) adducts.

For the compound with untethered nucleotides, (*cis*-1,4-DACH)Pt(5′-GMP)$_2$, as mentioned above, the HT conformation is favoured over HH.[65] Conversely, the overall data obtained at −10 °C confirm that, at this temperature, the more favoured conformation of the (*cis*-1,4-DACH)Pt(d(GpG)) adduct is HH1. Undoubtedly, the tethering of the two guanines by the sugar-phosphate backbone plays a key role in stabilising this HH conformation.

The same sample ((*cis*-1,4-DACH)Pt(d(GpG)) in D_2O–CD_3OD 2 : 1, v/v) was used to perform ^{31}P NMR experiments at different temperatures (Fig. 4). By lowering the temperature, the broad ^{31}P NMR signal at ∼−2 ppm observed at 25 °C decoalesces and, at the lowest temperature reached in the experiment (−10 °C), splits into one sharp signal at −2.20 ppm and a broad, weak, signal slightly more upfield. The sharp ^{31}P NMR signal at −2.20 ppm is compatible with those observed in water for HH1 conformers in other Pt(d(GpG)) adducts.[46,47,59] The more upfield signal is consistent with either a mixture of oligomeric Pt(d(GpG)) adducts with unstrained backbones (expected to have signals in this region) or with minor conformers of (*cis*-1,4-DACH)Pt(d(GpG)).

Table 1 ^{1}H NMR shifts (ppm) for the G residues in the HH1 conformer of (*cis*-1,4-DACH)Pt(oligo) adducts

	5′-G								3′-G							
Adduct	H8	H1′	H2′	H2″	H3′	H4′	H5′	H5″	H8	H1′	H2′	H2″	H3′	H4′	H5′	H5″
d(GpG)[a]	8.46	6.08	2.45	2.78	5.00	4.08	—	—	8.94	6.26	2.45	2.57	4.64	4.16	—	—
d(GGTTT)[b]	8.47	6.19	2.45	2.77	5.00	4.13	—	—	8.90	6.08	—	—	—	—	—	—
d(TGGT)[c]	8.29	6.29	2.48	2.88	5.38	4.33	4.08	4.12	9.24	6.30	2.78	2.48	5.37	4.53	4.25	4.08

[a] In D_2O–CD_3OD (2 : 1, v/v) at −10 °C. [b] In D_2O–CD_3OD (9 : 1, v/v) at −5 °C. [c] In D_2O at 5 °C.

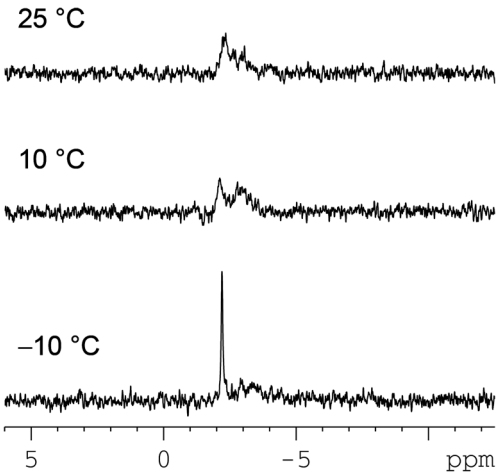

Fig. 4 ^{31}P NMR (242.93 MHz) spectra of the (*cis*-1,4-DACH)Pt(d(GpG)) adduct in D_2O–CD_3OD (2 : 1, v/v) at different temperatures.

Table 2 ^{13}C NMR shifts (ppm) for the (*cis*-1,4-DACH)Pt(d(GpG)) HH1 adduct in D_2O–CD_3OD (2 : 1, v/v) at −10 °C

G	C8	C1′	C2′	C3′	C4′
5′	138.7	82.8	38.6	71.1	85.5
3′	139.1	83.2	40.6	71.5	86.6

In order to assign the ^{13}C NMR signals of the postulated (*cis*-1,4-DACH)Pt(d(GpG)) HH1 conformer, a [^{1}H, ^{13}C] HSQC experiment was performed at −10 °C. The observed 3′- and 5′-G C8 signals were almost coincident (139.1 and 138.7 ppm, respectively; Table 2). Very similar chemical shifts were also found for the C1′ and C3′ atoms belonging to the two residues, whereas the largest differences between the 3′-G and 5′-G residues were observed for the C2′ ($\Delta\delta$ = 2.0 ppm) and C4′ ($\Delta\delta$ = 1.1 ppm) atoms. Similar differences have been observed for the HH1 conformer in retro-model studies of d(GpG) adducts.[46] The broad ^{1}H/^{13}C cross-peaks at 3.35/47.5 and 1.85/22.5 ppm in the [^{1}H,^{13}C] HSQC spectrum can be assigned to the two methynic and eight methylenic protons of *cis*-1,4-DACH, respectively.

Correlation between high and low temperature H8 signals. The two major, rather sharp H8 signals observed at 55 °C (8.18 and 8.41 ppm) must be coalescence signals of 5′-G and 3′-G H8 residues of different conformers. How can these high temperature signals be correlated to the low temperature signals at 8.46 and 8.94 ppm (−10 °C, Fig. 2), which have been assigned, respectively, to 5′-G H8 and 3′-G H8 of a major HH1 conformer? In the fortunate case of the ((*S*,*R*,*R*,*S*)-Bip)Pt(oligo) adducts,[46,47,59] it was possible to observe initially (kinetically controlled composition) two abundant conformers in *ca.* 1 : 1 ratio, while over time one of the two decreased in concentration (to nearly zero) in favour of the other, which was the most stable (equilibrium composition). The initial two conformers of ((*S*,*R*,*R*,*S*)-Bip)Pt(oligo) were determined to be HH1 (dominant and increasing) and ΔHT1 (decreasing). In other cases, the ΔHT1 conformer is long-lived enough to be studied.[58,59] The ΔHT1 conformer almost invariably has two closely spaced, relatively upfield H8 signals at ∼7.8 ppm. The favoured HH1 conformer is always characterized as having widely spaced, downfield-shifted H8 signals with more variable shifts than those for the ΔHT1 conformer.

Guided by the results of past studies, we can explain the temperature dependence for the H8 signals (Fig. 2). We begin by estimating the time-averaged H8 shifts for a 1 : 1 composition of HH1 and ΔHT1 conformers undergoing fast interconversion. For the HH1 shifts we use the values measured for (*cis*-1,4-DACH)Pt(d(GpG)) at −10 °C (8.94 and 8.46 ppm, Fig. 2), where this conformer dominates. For the ΔHT1 conformer (which is related to the HH1 conformer by having a *syn* conformation of the 3′-G residue having the base flipped with respect to the 5′-G residue), we use the chemical shifts observed for (*S*,*R*,*R*,*S*-Bip)Pt(d(GpG)) (7.91 and 7.77 ppm for 3′-G and 5′-G, respectively).[59] This leads to estimated high temperature H8 shift values for (*cis*-1,4-DACH)Pt(d(GpG)) of 8.42 and 8.12 ppm for 3′-G and 5′-G, respectively. These two values are very close (average discrepancy of only 0.04 ppm) to the shifts observed at 55 °C (8.41 and 8.18 ppm). Such an agreement is surprisingly good, in light of the very different nature of the carrier ligand and the different solvent system. However, we want to point out that similar chemical shifts for the ΔHT1 conformer have been observed in adducts with completely different carrier ligands (such as in (*N*,*N*′-Me_2-piperazine)Pt(d(GpG))) for which the H8 chemical shifts were 7.90 and 7.78 ppm for 3′-G and 5′-G, respectively.[60] Moreover, the chemical shifts are expected to be very little affected by the composition of the solvent in the case of a water and methanol mixture. Therefore, we can be confident that the high temperature spectrum reflects the coalescence set of signals of two dominating conformers, HH1 and ΔHT1 (and possibly some minor conformers). We can deduce that, at high temperature, the 3′-G can rapidly flip between the HH and HT orientations with respect to the 5′-G.

We turn now to the effect on H8 signals of lowering the temperature from 55 °C to −10 °C (Fig. 2). The equilibrium position will begin to favour the HH1 conformer, and the rate of 3′-G flipping will slow. Such a process will only slightly affect the chemical shift of the 5′-G H8 signal because this guanine is L canted in HH1, and the H8 is already in the shielding cone of the 3′-G, as it is in the ΔHT1 conformer. Therefore, the broadening of the 5′-G H8 signal will be moderate, as observed. In contrast, the flipping of 3′-G will strongly affect the 3′-G H8 signal, which is deshielded by the L-canted *cis* 5′-G base in the HH1 conformer but is shielded by the *cis* G in the ΔHT1 conformer. Therefore, the resulting large changes in H8 chemical shift with temperature will lead to more pronounced broadening of 3′-G H8 signal. A similar explanation for changes in shift has been proposed by Kozelka *et al.* for the (*N*,*N*,*N*′-trimethylethylenediamine)Pt(d(GpG)) adduct.[93] Thus, the spectral changes observed for the (*cis*-1,4-DACH)Pt(d(GpG)) adduct can be rationalized by the presence of two dominant conformers, HH1 and ΔHT1, in rapid interconver-

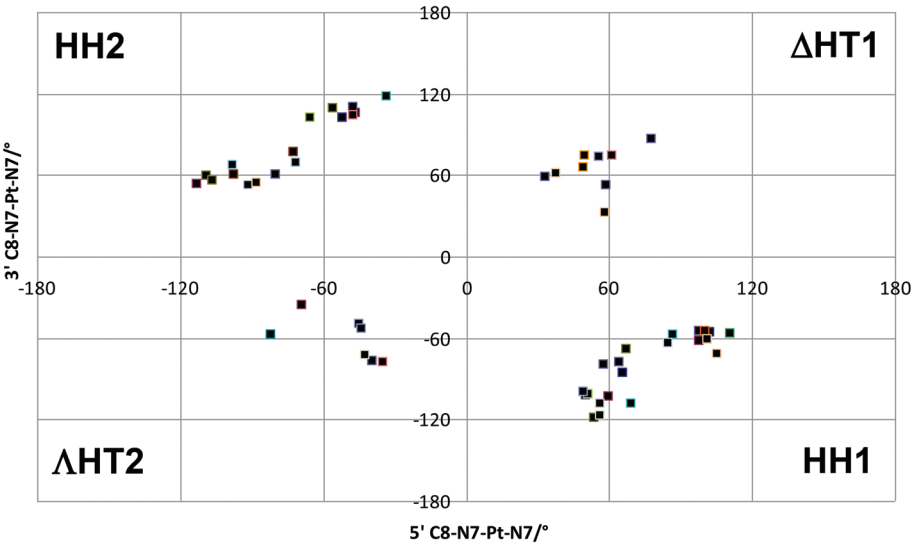

Fig. 5 Scatter plot of 3′ C8–N7–Pt–N7 *vs.* 5′ C8–N7–Pt–N7 torsion angles found in conformational search.

sion at high temperature and by a decrease in the rate of interconversion and a change in the equilibrium composition greatly favouring the HH1 conformer upon lowering the temperature. However, a small abundance of the ΔHT1 conformer in moderately fast exchange with the HH1 conformer cannot be ruled out because this situation will not significantly broaden the HH1 H8 signals, and broad, weak ΔHT1 signals would escape detection. A small abundance of the ΔHT1 conformer in the dynamic equilibrium would explain the non-negligible H8–H1′ NOE cross-peak observed for 3′-G in the (*cis*-1,4-DACH)Pt(d(GpG)) adduct. A strong H8–H1′ NOE is observed for 3′-G in ΔHT1 conformers because of the *syn* conformation of the 3′-G residue.[58–60,64,96]

Theoretical calculations. Theoretical calculations were performed on (*cis*-1,4-DACH)Pt(d(GpG)) to explore possible conformations in more detail. Starting from the PM6-DH2 optimised geometry of an HH1 conformation, a stochastic conformational search for all rotatable bonds was performed. This procedure led to 54 conformations that, when plotted according to their C8–N7–Pt–N7 torsion angles, clearly fall into four distinct families of conformations corresponding to two HH and two HT groups (Fig. 5). In total 21 HH1, 17 HH2, 9 ΔHT1 and 7 ΛHT2 conformations were located. The lowest-energy structure located in this search corresponds to an HH2 conformation with the 5′-G residue in an *anti* conformation and the 3′-G residue in the *syn* conformation, and the next two lowest energy conformers were also classed as HH2. The first HH1 form was found 1 kcal mol^{-1} higher in energy than the global minimum, the first ΛHT2 form at 1.5 kcal mol^{-1}, and the first ΔHT1 at 7.3 kcal mol^{-1}. Thus, while this analysis supports the finding that this complex is conformationally flexible, and the speed of the LFMM method allows efficient exploration of conformational space of such a complex, the details of specific conformations found to have low energy do not agree with experimental observations.

This lack of agreement with experimental data led us to look in more detail at structures and energies, since the molecular mechanics formalism used may not reflect all the subtleties of conformational freedom in these systems. All 54 conformations were therefore re-optimised using the semi-empirical PM6-DH2 method, in both gas-phase and simulated aqueous solvent, with a Na^+ ion placed in the proximity of the phosphate group. It was found that MM and PM6-DH2 energies are almost completely unrelated (R^2 = 0.007), with high energy conformers from the former method becoming amongst the lowest energy forms after re-optimization with the latter. The energy of the most stable PM6-DH2 structure from each family is reported in Table 3, and confirms that these predictions are quite different from those of MM. In both the gas and aqueous phases, an HH1 conformer is found to be the most stable of all 54 conformations considered. The HH2 form is much higher in energy, while both HT forms are lower than HH2 but significantly less stable than the global minimum.

Thus the PM6-DH2 calculations correctly show that, after HH1, ΔHT1 is the most preferred conformation. Correction of the values in Table 3 for thermal and entropy effects at a range of temperatures similar to those used for NMR experiments had essentially no effect on the energy order.

Table 3 Relative energies of (*cis*-1,4-DACH)Pt(d(GpG)) adduct conformations (kcal mol^{-1})

	PM6-DH2	
	Gas-phase	Aqueous-phase
HH1	0.0	0.0
HH2	22.8	21.6
ΛHT2	14.2	5.9
ΔHT1	8.2	5.8

The PM6-DH2 optimised HH1 geometry has both guanines in their *anti*-form, whereas the lowest energy ΔHT1 form has 5′-G in *anti*- and 3′-G in *syn*-forms; therefore a fast interconversion between HH1 and ΔHT1 (even if ΔHT1 is present in small amounts at low temperature) can explain the NMR data showing a partial *syn* conformation for 3′-G.

Reaction with d(GGTTT)

The ^{1}H NMR spectrum of free d(GGTTT) in D_2O solution at pH ~ 4 consists of two G H8 (8.03 and 7.82 ppm, assigned to 3′-G and 5′-G, respectively) and three T H6 signals (7.68, 7.63, and 7.55 ppm). These signals dominate in the 10 min trace in Fig. S2 (ESI†). Addition of $[Pt(OD_2)_2(cis\text{-}1,4\text{-DACH})]^{2+}$ produces new signals in the 9–7 ppm region (Fig. S2†): two broad G H8 signals (8.52 and 8.25 ppm) and two resolved T H6 peaks (7.66 and 7.63 ppm, integrating for 2 protons and 1 proton, respectively). The downfield shift of the G H8 signals is consistent with coordination of both G residues to Pt to form the (*cis*-1,4-DACH)Pt(d(GGTTT)) adduct.

Temperature effect. Upon raising the temperature (40 °C), the two broad H8 signals of (*cis*-1,4-DACH)Pt(d(GGTTT) at 25 °C (Fig. 6) become sharper and shift slightly upfield (to 8.48 and 8.22 ppm); the difference in chemical shift ($\Delta\delta$ = 0.26 ppm) remains almost unchanged when compared to that at 25 °C. Bringing the reaction mixture back to 25 °C restores the initial spectrum with the two broad H8 signals. Upon lowering the temperature, the two broad H8 signals first merge into a single, very broad feature (15 °C) and then sharpen again, giving (at 5 °C) two clear H8 signals at 8.40 and 8.80 ppm. (A broader feature around 8.20 ppm, still present, probably belongs to oligomeric platinum adducts.)

In order to be able to lower the temperature even further, we added some methanol to the sample solution (D_2O–CD_3OD 9 : 1, v/v) and recorded the ^{1}H NMR spectrum at −5 °C (Fig. 6), which showed the G H8 signals shifted further downfield (to 8.47 and 8.90 ppm). In the 2D NOESY spectrum recorded at −5 °C (Fig. 7), the two H8 signals exhibit a cross-peak indicative of an HH arrangement of the G bases. The more upfield H8 signal (8.47 ppm; Table 1) has H8–H2′/H2″ NOE cross-peaks, while the H8–H1′ NOE cross-peak is weak; both features are indicative of an *anti* nucleotide conformation. Moreover, an H8–H3′ cross-peak is consistent with an N-sugar pucker characteristic of a 5′-G residue.[46] Thus, the more upfield H8 signal can be assigned to 5′-G. The more downfield H8 signal at 8.90 ppm (Table 1) shows complete absence of an H8–H3′ NOE cross peak, indicative of an S-sugar pucker characteristic of a 3′-G residue.[91] Thus the downfield H8 signal must belong to 3′-G. In this case there is quite an intense H8–H1′ cross-peak. The presence of a H8–H1′ cross-peak indicates either a partial *syn* character[58–60,64,91,94] for the 3′-G of the dominant conformer or, more likely, the existence of a minor ΔHT1 conformer in dynamic equilibrium with the dominant HH1 conformer. Such a dynamic equilibrium would explain the somewhat broad nature of the H8 signals, even at −5 °C (Fig. 6). An upfield 5′-G H8 signal is indicative of a left-hand

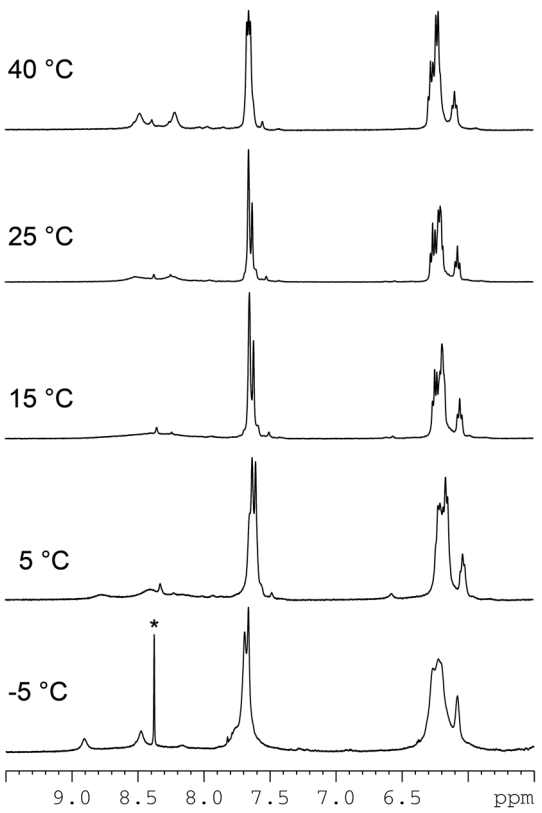

Fig. 6 Temperature dependence of the downfield region of the ^{1}H NMR (400 MHz) spectrum of (*cis*-1,4-DACH)Pt(d(GGTTT)) in D_2O solution (pH ~ 4). The spectrum at −5 °C was recorded after addition of methanol to the sample solution (D_2O–CD_3OD 9 : 1, v/v). The asterisk indicates an impurity present in the solvent (likely formate from plastic pipette tips).

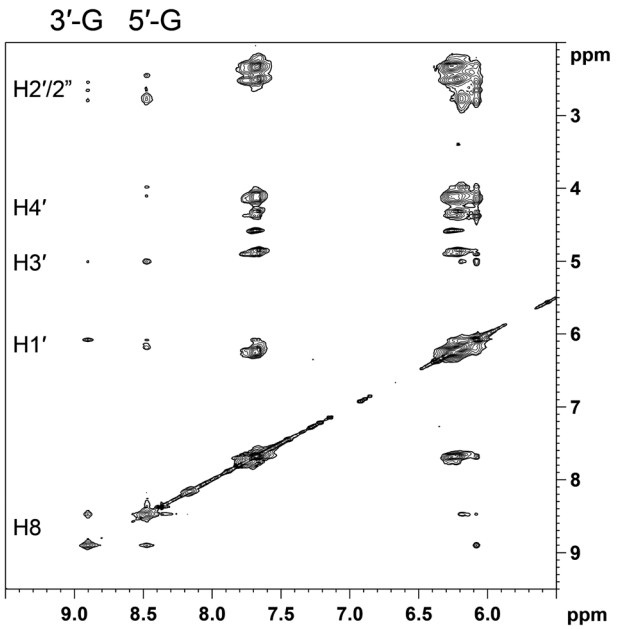

Fig. 7 Selected region of the 2D NOESY spectrum (700 MHz) obtained for (*cis*-1,4-DACH)Pt(d(GGTTT)) in D_2O–CD_3OD (9 : 1, v/v) at −5 °C.

Table 4 ^{31}P NMR shifts (ppm) for free d(GGTTT) and (*cis*-1,4-DACH)Pt-(d(GGTTT)) at 25 °C

	GpG	GpT	TpTpT
d(GGTTT)	−4.17	−4.17	−4.25
(*cis*-1,4-DACH)Pt(d(GGTTT))	−3.54	−4.18	−4.29

canting of the 5′-G, as expected for a *cis*-A_2Pt(ss-oligo) adduct.[5,6,27,31,33,34,43]

Free d(GGTTT) at 25 °C consists of two overlapping ^{31}P NMR signals at −4.17 ppm and a third signal at −4.25 ppm. Complexation to platinum causes broadening and shift to lower field (−3.54 ppm) of one ^{31}P NMR signal (undoubtedly arising from the phosphodiester group connecting the two cross-linked G's, Fig. S3 in the ESI† and Table 4). The value of the ^{31}P NMR chemical shift of the GpG signal (−3.54 ppm) lies between the values typically found for the HH1 (∼−3 ppm) and the ΔHT1 conformer (∼−5 ppm).[17,59] Moreover, the broadness of the GpG ^{31}P signal indicates that there is interconversion between conformers at a rate comparable to the NMR time scale.

Overall, the behaviour of (*cis*-1,4-DACH)Pt(d(GGTTT)) appears to be very similar to that of (*cis*-1,4-DACH)Pt(d(GpG)), as expected from our retro-modelling studies on short oligos differing only in the presence of additional residues in the 3′ position.[46,47] In both d(GpG) and d(GGTTT) adducts, the absence of additional residues in the 5′ position is consistent with our previous finding that other conformers in addition to HH1 are possible.[47,59] In the cases in which the adducts are not dynamic, we have established that the next most favoured conformer is ΔHT1.[58] This interpretation of a rapidly interconverting HH1/ΔHT1 conformer mixture, with ΔHT1 becoming less abundant at lower temperature, explains the temperature dependence of the G H8 signals between 5 °C and 40 °C, as discussed above for the (*cis*-1,4-DACH)Pt(d(GpG)) adduct. The *syn* conformation of the 3′-G residue of the ΔHT1 conformer is well documented;[46,58] a small amount of the ΔHT1 conformer can explain the observation of a significant H8–H1′ cross-peak in the 2D NOESY spectrum at −5 °C (Fig. 7).

Reaction with d(TGGT)

The progress of the reaction between $[Pt(OD_2)_2$(*cis*-1,4-DACH)$]^{2+}$ and d(TGGT) (room temperature, pH ∼ 4) was monitored by ^{1}H NMR spectroscopy (Fig. S4 in the ESI†). Initially, the ^{1}H NMR spectrum (5–10 ppm region) showed only the signals of free d(TGGT) (singlets at 8.00, 7.90, 7.54, and 7.43 ppm assigned to 3′-G H8, 5′-G H8, 3′-T H6, and 5′-T H6, respectively; and doublets of doublets falling at 6.23, 6.13, 6.06, and 5.89 ppm assigned to H1′ protons of 3′-T, 3′-G, 5′-G, and 5′-T, respectively. The numbering scheme of d(TGGT) is shown in Fig. S5 of the ESI†).[33,46,47] After 1 day, a new set of signals was observed in the aromatic region; after 26 days this new set became exclusive, indicating that the reaction had reached completion. The downfield shift of the G H8 signals in the new set of signals indicates formation of a (*cis*-1,4-DACH)Pt(d(TGGT)) adduct, in which the Pt atom is coordinated to the adjacent G residues. As for the H8 signals of the G residues, the H6 signals of the T residues and the H1′ signals were also shifted to lower field. Importantly, unlike our findings for (*cis*-1,4-DACH)Pt(d(GpG)) and (*cis*-1,4-DACH)Pt-(d(GGTTT)), the H8 signals of the (*cis*-1,4-DACH)Pt(d(TGGT)) adduct show little broadening.

The complete assignment of the signals for the non-exchangeable base and sugar protons of the two G's in the (*cis*-1,4-DACH)Pt(d(TGGT)) adduct was accomplished through 2D COSY and NOESY spectra (Table 1). In particular, the 2D NOESY spectrum recorded at 5 °C (Fig. 8) showed a NOE cross-peak between the two sharp H8 signals, which is indicative of an HH conformer. The more upfield H8 signal (8.29 ppm, Table 1) showed H8–H2′/H2″ cross-peaks but no detectable H8–H1′ NOE cross-peak; both features are characteristic of an *anti* conformation.[91,95,96] Moreover, a strong H8–H3′ cross-peak is consistent with an N sugar pucker,[26,31,91] characteristic of a 5′-G residue in an intrastrand cross-link.[5,8,17,58–60,64] The more downfield H8 signal (9.24 ppm; Table 1) showed strong H8–H2′/H2″ cross-peaks and a nearly undetectable H8–H1′ cross-peak, which are indicative of an *anti* residue.[91,95,96] Moreover, the complete absence of an H8–H3′ cross-peak suggests that the sugar of this residue retains the S pucker;[91] therefore, these signals are assigned to the 3′-G residue because the S pucker is characteristic of the 3′-G residue. As found for (*cis*-1,4-DACH)Pt(d(GpG)) and (*cis*-1,4-DACH)Pt(d(GGTTT)), the (*cis*-1,4-DACH)Pt(d(TGGT)) adduct also has an upfield 5′-G H8 signal indicative of L canting of the 5′-G, a common feature of *cis*-A_2Pt(ss-oligo) adducts.

The ^{31}P NMR spectrum of (*cis*-1,4-DACH)Pt(d(TGGT)), taken at 25 °C, consists of three signals at −2.95, −4.09, and

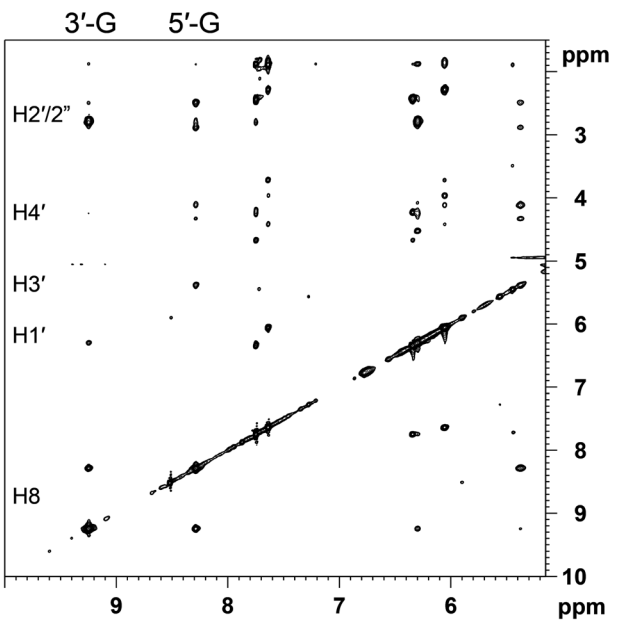

Fig. 8 Selected region of the 2D NOESY (600 MHz) spectrum obtained for (*cis*-1,4-DACH)Pt(d(TGGT)) in D_2O at 5 °C.

Table 5 ^{31}P NMR shifts (ppm) for d(TGGT) and (*cis*-1,4-DACH)Pt-(d(TGGT)) at 25 °C

	GpG	GpT	TpG
d(TGGT)	−4.14	−4.20	−4.09
(*cis*-1,4-DACH)Pt(d(TGGT))	−2.95	−4.09	−4.17

−4.17 ppm (Fig. S6 in the ESI†). The ^{31}P NMR chemical shifts for free and complexed d(TGGT) are listed in Table 5; the large downfield change in chemical shift of the GpG phosphodiester group (from −4.14 ppm in free d(TGGT) to −2.95 ppm in the (*cis*-1,4-DACH)Pt(d(TGGT)) adduct) confirms that the adduct exists mostly in the HH1 conformation.[17,31,60,64]

Temperature effect. The effect of temperature on the ^{1}H (Fig. 9) and ^{31}P NMR spectra (Fig. S7 in the ESI†) of (*cis*-1,4-DACH)Pt(d(TGGT)) (D_2O solution) was also investigated. At 25 °C the 3′-G H8 signal (9.06 ppm) is broad and 0.86 ppm downfield with respect to the 5′-G H8 signal (8.20 ppm).

Raising the temperature caused the 3′-G H8 signal of (*cis*-1,4-DACH)Pt(d(TGGT)) to shift upfield (from 9.06 ppm at 25 °C to 9.00 ppm at 40 °C), while the 5′-G H8 signal shifted downfield (from 8.20 ppm at 25 °C to 8.22 ppm at 40 °C), and the separation between the two resonances decreased from 0.86 (25 °C) to 0.78 ppm (40 °C) (Fig. 9; Table S1 in the ESI†). Moreover, both the 3′-G and 5′-G H8 signals became sharper.

Lowering the temperature to 5 °C resulted in further deshielding of the 3′-G H8 signal (9.15 ppm), which became sharper and was farther (0.98 ppm) from the 5′-G H8 signal (8.17 ppm). The separation between the two H8 resonances was larger at 5 °C than at 25 °C (Fig. 9, Table S1†). These data suggest that in solution a major conformer (probably the HH1 conformer) is in equilibrium with another conformer (probably the ΔHT1 conformer) whose concentration (unlike the d(GpG) and the d(GGTTT) cases) always remains low, as judged by the small shift and change of peak sharpness with the temperature (estimated ~5% ΔHT1). In retro-model studies, the minor ΔHT1 conformer has been shown to have a low abundance when there is a residue on the 5′-G.[46,47] At 5 °C the interconversion between the two conformers is slower than at 25 °C, which could explain both the sharpening of the downfield H8 signal of the dominating conformer and the increased separation between the two H8 signals. Therefore, because the downfield signal of the dominating conformer has its counterpart resonance (in the low-percent ΔHT1 conformer) falling at much higher field, a lowering of the interconversion rate between conformers will have a greater effect (both in terms of sharpness and chemical shift) on the downfield signal than on the upfield signal, for which the chemical shift is close to that of its counterpart in the low-percent conformer. The low abundance of the ΔHT1 conformer and its slow exchange with the major HH1 conformer are also consistent with the very weak H8–H1′ NOE cross-peak observed for the 3′-G residue, which has the *anti* conformation in the dominant HH1 conformer.

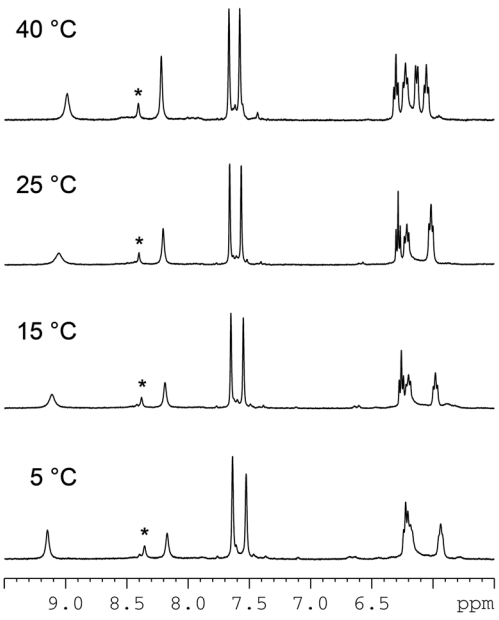

Fig. 9 Temperature dependence of the downfield portion of the ^{1}H NMR (400 MHz) spectrum of (*cis*-1,4-DACH)Pt(d(TGGT)) in D_2O (pH ~ 4). The asterisk indicates an impurity of the sample (likely formate from plastic pipette tips).

The 5′-G H1′ signal of (*cis*-1,4-DACH)Pt(d(TGGT)) was also affected by temperature (Fig. S8 in the ESI†). At 25 °C this signal overlapped with other H1′ signals (see also Fig. 9). When the temperature was raised from 25 to 40 °C, the 5′-G H1′ signal shifted downfield (Fig. S8), and the 40 °C spectrum showed the signal as a doublet ($J_{1'-2'}$ < 0.5 Hz and $J_{1'-2''}$ = 7.17 Hz), confirming an N-type ribose conformation. However, at lower temperatures the 5′-G H1′ signal shifted upfield and broadened to such an extent that below 15 °C it was lost in the base line. The other H1′ signals, in contrast, underwent little shift. This unusual behaviour has been observed with other adducts,[33] and thus we conclude that the sugar-phosphate backbone in (*cis*-1,4-DACH)Pt(d(TGGT)) is representative of the backbone in other adducts.

The TGpGT ^{31}P signal was not strongly affected by temperature; however, increasing the temperature from 5 to 40 °C shifted the TGpGT ^{31}P signal from −3.03 to −2.87 ppm (Fig. S7, Table S2†). These values also indicate that the backbone is similar to that in other adducts.[33]

Compared to (*cis*-1,4-DACH)Pt(d(GpG)) and (*cis*-1,4-DACH)-Pt(d(GGTTT)) adducts, the presence of a 5′ residue flanking the coordinated 5′-G in (*cis*-1,4-DACH)Pt(d(TGGT)) is responsible for the small abundance of the HT conformer found even at high temperature and, as a consequence, the small changes of H8 chemical shifts as a function of temperature. This 5′-substituent effect favouring the HH1 conformer is well documented.[46,47,61] This finding is further evidence that (*cis*-1,4-DACH)-Pt(d(TGGT)) is representative of many d(TGGT) adducts with several other carrier ligands used in retro-modelling studies. Although as extensive a study of temperature effects was not conducted for the d(TGGT) adduct derived from cisplatin, this latter adduct has H8 signals at 9.04 ppm (3′-G) and 8.25 ppm

(5′-G) at 22 °C and a ^{31}P NMR signal at −3.02 ppm at 15 °C.[33] It is noteworthy that these values are almost identical to those found here [9.06 ppm (3′-G H8), 8.20 ppm (5′-G H8) and GpG ^{31}P NMR signal at −2.95 ppm at 25 °C] for the (*cis*-1,4-DACH)-Pt(d(TGGT)) adduct. For both the cisplatin and the Kiteplatin adducts, the GpG ^{31}P NMR signal shifts slightly upfield with temperature.

Conclusions

In the present work the behaviour of (*cis*-1,4-DACH)Pt(d(GpG)), (*cis*-1,4-DACH)Pt(d(GGTTT)), and (*cis*-1,4-DACH)Pt(d(TGGT)) adducts has been investigated by ^{1}H and ^{31}P NMR spectroscopy and compared to that of related cross-link adducts of these same short DNA fragments but with more bulky and less bulky carrier ligands. From this direct comparison of adducts, we conclude that the carrier ligand present in Kiteplatin, *cis*-1,4-DACH, influences the dynamic properties much more than the less bulky carrier ligands but much less than more bulky carrier ligands. The new results indicate that bulk is much less important in influencing the equilibrium or structural properties of adducts.

The shifts of the ^{1}H and ^{31}P NMR signals reflect values found with highly dynamic adducts having less bulky carrier ligands associated with anticancer activity. At 25 °C and at somewhat elevated temperatures, NMR signals are broad, unlike the sharp signals observed for adducts with cisplatin or with other primary amines. We conclude that the very large bite angle of *cis*-1,4-DACH, coupled with the rigid frame of the chelating cyclohexane ring inserted in the 7-member chelate, slows down the interconversion between different conformers in (*cis*-1,4-DACH)Pt(ss-oligo) cross-linked adducts. Thus, the *cis*-1,4-DACH ligand is a very valuable and informative carrier ligand because it has allowed us to detect evidence for the coexistence of different conformers in a system containing a primary diamine carrier ligand associated with anticancer activity. Furthermore, the results from adducts with the *cis*-1,4-DACH ligand, which is relatively non-bulky, confirm the previous hypothesis that the coexistence of different conformers established in studies of retro models that have relatively bulky ligands is not an artefact resulting from carrier-ligand bulk.[94]

At close to the physiological temperature (40 °C), the ^{1}H and ^{31}P NMR data for the (*cis*-1,4-DACH)Pt(d(GpG)) and (*cis*-1,4-DACH)Pt(d(GGTTT)) adducts indicate a mixture of comparable amounts of mostly HH1 and ΔHT1 conformers. In contrast, the data for the (*cis*-1,4-DACH)Pt(d(TGGT)) adduct indicate that, even at high temperature, there is one major, highly dominant conformer (HH1), and any ΔHT1 conformer present has a very small concentration, thus causing only a minimal broadening of the H8 NMR signals. This result is fully consistent with findings for adducts with many different bulky carrier ligands, in which the effect of 5′-substituents on the 5′-G of the cross-link is to favour the normal HH1 conformer.

At low temperature (close to 0 °C), our results are unique because they show that for the (*cis*-1,4-DACH)Pt(d(GpG)) and (*cis*-1,4-DACH)Pt(d(GGTTT) adducts, the equilibrium between HH1 and ΔHT1 conformers (present in comparable amounts at 40 °C) shifts dramatically toward the more stable HH1 conformer. (A very small shift was observed for the (*cis*-1,4-DACH)-Pt(d(TGGT)) adduct for which the HH1 conformer was already dominant at high temperature.)

Conformational searching using ligand field molecular mechanics (LFMM), performed on the d(GpG) adduct, located four families of conformations, the lowest energy of which corresponded to an HH2 conformer with *syn* and *anti* conformations for 3′-G and 5′-G residues, respectively. In contrast, semi-empirical PM6-DH2 studies predicted the HH1 conformer to be lowest in energy in the gas phase as well as in aqueous solution. The PM6-DH2 calculations also correctly show that, after HH1, ΔHT1 is the most preferred conformation. Furthermore, the calculations confirmed that the 3′-G residue has *anti* conformation in HH1 while it has *syn* conformation in ΔHT1; therefore, a rapid interconversion between HH1 and ΔHT1 (even if ΔHT1 is present in small amounts at low temperature) can explain the NMR data showing a partial *syn* conformation for 3′-G.

Because the bulk of the *cis*-1,4-DACH carrier ligand does not have a dramatic effect on conformer stability or structure, the main local effect of the ligand, namely the impeded rotation of the guanine bases with respect to the Pt–N7 bond, could contribute to the markedly different biological activity of kiteplatin[69–71] as compared to those of cisplatin and oxaliplatin.[69–71,79] Alternatively, and perhaps more likely, the shape and bulk of the carrier ligand, as it projects out away from the DNA helix, will influence interactions with nucleic acid binding proteins or repair enzymes, thereby influencing activity.

Acknowledgements

We acknowledge the University of Bari (Italy), the Italian Ministero dell'Università e della Ricerca (FIRB RINAME RBAP114AMK and PON02_00607_3621894), the Inter-University Consortium for Research on the Chemistry of Metal Ions in Biological Systems (C.I.R.C.M.S.B.), and the European Union (COST CM1105: Functional metal complexes that bind to biomolecules) for support.

References

1 M. J. Bloemink and J. Reedijk, in *Metal Ions in Biological Systems*, ed. A. Sigel and H. Sigel, Marcel Dekker, New York, 1996, vol. 32, pp. 641–685.
2 J. Reedijk, *Chem. Commun.*, 1996, 801–806.
3 S. E. Sherman and S. J. Lippard, *Chem. Rev.*, 1987, **87**, 1153–1181.

4 J.-C. Chottard, J.-P. Girault, G. Chottard, J.-Y. Lallemand and D. Mansuy, *J. Am. Chem. Soc.*, 1980, **102**, 5565–5572.
5 J. H. J. den Hartog, C. Altona, J.-C. Chottard, J.-P. Girault, J.-Y. Lallemand, F. A. de Leeuw, A. T. M. Marcelis and J. Reedijk, *Nucleic Acids Res.*, 1982, **10**, 4715–4730.
6 J.-P. Girault, G. Chottard, J.-Y. Lallemand and J.-C. Chottard, *Biochemistry*, 1982, **21**, 1352–1356.
7 J. Kozelka, M. H. Fouchet and J.-C. Chottard, *Eur. J. Biochem.*, 1992, **205**, 895–906.
8 S. E. Sherman, D. Gibson, A. Wang and S. J. Lippard, *J. Am. Chem. Soc.*, 1988, **110**, 7368–7381.
9 D. Yang, S. van Boom, J. Reedijk, J. van Boom and A. Wang, *Biochemistry*, 1995, **34**, 12912–12920.
10 G. Natile and L. G. Marzilli, *Coord. Chem. Rev.*, 2006, **250**, 1315–1331.
11 S. O. Ano, Z. Kuklenyik and L. G. Marzilli, in *Cisplatin: Chemistry and Biochemistry of a Leading Anticancer Drug*, ed. B. Lippert, Wiley-VCH, Weinheim, 1999, pp. 247–291.
12 F. Coste, J.-M. Malinge, L. Serre, W. Shepard, M. Roth, M. Leng and C. Zelwer, *Nucleic Acids Res.*, 1999, **27**, 1837–1846.
13 H. Huang, L. Zhu, G. P. Drobny, P. B. Hopkins and B. R. Reid, *Science*, 1995, **270**, 1842–1845.
14 F. Paquet, C. Perez, M. Leng, G. Lancelot and J.-M. Malinge, *J. Biomol. Struct. Dyn.*, 1996, **14**, 67–77.
15 A. L. Pinto and S. J. Lippard, *Biochim. Biophys. Acta*, 1985, **780**, 167–180.
16 J. L. van der Veer and J. Reedijk, *Chem. Br.*, 1988, **24**, 775–780.
17 S. O. Ano, F. P. Intini, G. Natile and L. G. Marzilli, *J. Am. Chem. Soc.*, 1998, **120**, 12017–12022.
18 T. P. Kline, L. G. Marzilli, D. Live and G. Zon, *J. Am. Chem. Soc.*, 1989, **111**, 7057–7068.
19 J. H. J. den Hartog, C. Altona, J. H. van Boom, G. A. van der Marel, C. A. G. Haasnoot and J. Reedijk, *J. Biomol. Struct. Dyn.*, 1985, **2**, 1137–1155.
20 F. Herman, J. Kozelka, V. Stoven, E. Guittet, J.-P. Girault, T. Huynh-Dinh, J. Igolen, J.-Y. Lallemand and J.-C. Chottard, *Eur. J. Biochem.*, 1990, **194**, 119–133.
21 D. Yang, S. S. G. E. van Boom, J. Reedijk, J. H. van Boom and A. H.-J. Wang, *Biochemistry*, 1995, **34**, 12912–12920.
22 J. H. J. den Hartog, C. Altona, J. H. van Boom and J. Reedijk, *FEBS Lett.*, 1984, **176**, 393–397.
23 A. Gelasco and S. J. Lippard, *Biochemistry*, 1998, **37**, 9230–9239.
24 J. H. J. den Hartog, C. Altona, J. H. van Boom, G. A. van der Marel, C. A. G. Haasnoot and J. Reedijk, *J. Am. Chem. Soc.*, 1984, **106**, 1528–1530.
25 B. van Hemelrych, E. Guittet, G. Chottard, J.-P. Girault, F. Herman, T. Huynh-Dinh, J.-Y. Lallemand, J. Igolen and J.-C. Chottard, *Biochem. Biophys. Res. Commun.*, 1986, **138**, 758–763.
26 L. G. Marzilli, J. Saad, Z. Kuklenyik, K. A. Keating and Y. Xu, *J. Am. Chem. Soc.*, 2001, **123**, 2764–2770.
27 J. H. J. den Hartog, C. Altona, G. A. van der Marel and J. Reedijk, *Eur. J. Biochem.*, 1985, **147**, 371–379.
28 S. K. Miller and L. G. Marzilli, *Inorg. Chem.*, 1985, **24**, 2421–2425.
29 M. D. Reily and L. G. Marzilli, *J. Am. Chem. Soc.*, 1986, **108**, 6785–6793.
30 S. J. Berners-Price, K. J. Barnam, U. Frey and P. J. Sadler, *Chem. – Eur. J.*, 1996, **2**, 1283–1291.
31 S. Mukundan Jr., Y. Xu, G. Zon and L. G. Marzilli, *J. Am. Chem. Soc.*, 1991, **113**, 3021–3027.
32 S. S. G. E. van Boom, D. Yang, J. Reedijk, G. A. van der Marel and A. H.-J. Wang, *J. Biomol. Struct. Dyn.*, 1996, **13**, 989–998.
33 C. S. Fouts, L. G. Marzilli, R. A. Byrd, M. F. Summers, G. Zon and K. Shinozuka, *Inorg. Chem.*, 1988, **27**, 366–376.
34 J. L. van der Veer, G. A. van der Marel, H. van den Elst and J. Reedijk, *Inorg. Chem.*, 1987, **26**, 2272–2275.
35 S. U. Dunham and S. J. Lippard, *J. Am. Chem. Soc.*, 1995, **117**, 10702–10712.
36 T. W. Hambley, E. C. H. Ling and B. A. Messerle, *Inorg. Chem.*, 1996, **35**, 4663–4668.
37 F. Gonnet, F. Reeder, J. Kozelka and J.-C. Chottard, *Inorg. Chem.*, 1996, **35**, 1653–1658.
38 A. T. M. Marcelis, J. H. J. den Hartog, G. A. van der Marel, G. Wille and J. Reedijk, *Eur. J. Biochem.*, 1983, **135**, 343–349.
39 J.-M. Neumann, S. Tran-Dinh, J.-P. Girault, J.-C. Chottard and T. Huynh-Dinh, *Eur. J. Biochem.*, 1984, **141**, 465–472.
40 R. A. Byrd, M. F. Summers, G. Zon, C. S. Fouts and L. G. Marzilli, *J. Am. Chem. Soc.*, 1986, **108**, 504–505.
41 M. J. Bloemink, R. J. Heetebrij, K. Inagaki, Y. Kidani and J. Reedijk, *Inorg. Chem.*, 1992, **31**, 4656–4661.
42 C. J. van Garderen, M. J. Bloemink, E. Richardson and J. Reedijk, *J. Inorg. Biochem.*, 1991, **42**, 199–205.
43 S. J. Berners-Price, J. D. Ranford and P. J. Sadler, *Inorg. Chem.*, 1994, **33**, 5842–5846.
44 D. P. Bancroft, C. A. Lepre and S. J. Lippard, *J. Am. Chem. Soc.*, 1990, **112**, 6860–6871.
45 M.-H. Fouchet, E. Guittet, J. A. H. Cognet, J. Kozelka, C. Gauthier, M. Le Bret, K. Zimmermann and J.-C. Chottard, *J. Biol. Inorg. Chem.*, 1997, **2**, 83–92.
46 J. S. Saad, G. Natile and L. G. Marzilli, *J. Am. Chem. Soc.*, 2009, **131**, 12314–12324.
47 J. S. Saad, P. A. Marzilli, F. P. Intini, G. Natile and L. G. Marzilli, *Inorg. Chem.*, 2011, **50**, 8608–8620.
48 S. O. Ano, F. P. Intini, G. Natile and L. G. Marzilli, *Inorg. Chem.*, 1999, **38**, 2989–2999.
49 L. G. Marzilli, F. P. Intini, D. Kiser, H. C. Wong, S. O. Ano, P. A. Marzilli and G. Natile, *Inorg. Chem.*, 1998, **37**, 6898–6905.
50 H. C. Wong, R. Coogan, F. P. Intini, G. Natile and L. G. Marzilli, *Inorg. Chem.*, 1999, **38**, 777–787.
51 H. C. Wong, F. P. Intini, G. Natile and L. G. Marzilli, *Inorg. Chem.*, 1999, **38**, 1006–1014.
52 S. T. Sullivan, A. Ciccarese, F. P. Fanizzi and L. G. Marzilli, *Inorg. Chem.*, 2000, **39**, 836–842.
53 S. O. Ano, F. P. Intini, G. Natile and L. G. Marzilli, *J. Am. Chem. Soc.*, 1997, **119**, 8570–8571.

54 J. S. Saad, T. Scarcia, G. Natile and L. G. Marzilli, *Inorg. Chem.*, 2002, **41**, 4923–4935.
55 J. S. Saad, T. Scarcia, K. Shinozuka, G. Natile and L. G. Marzilli, *Inorg. Chem.*, 2002, **41**, 546–557.
56 S. T. Sullivan, J. S. Saad, F. P. Fanizzi and L. G. Marzilli, *J. Am. Chem. Soc.*, 2002, **124**, 1558–1559.
57 N. Margiotta, P. Papadia, F. P. Fanizzi and G. Natile, *Eur. J. Inorg. Chem.*, 2003, 1136–1144.
58 J. S. Saad, M. Benedetti, G. Natile and L. G. Marzilli, *Inorg. Chem.*, 2011, **50**, 4559–4571.
59 L. G. Marzilli, S. O. Ano, F. P. Intini and G. Natile, *J. Am. Chem. Soc.*, 1999, **121**, 9133–9142.
60 S. T. Sullivan, A. Ciccarese, F. P. Fanizzi and L. G. Marzilli, *J. Am. Chem. Soc.*, 2001, **123**, 9345–9355.
61 S. T. Sullivan, J. S. Saad, F. P. Fanizzi and L. G. Marzilli, *J. Am. Chem. Soc.*, 2002, **124**, 1558–1559.
62 D. Bhattacharyya, P. A. Marzilli and L. G. Marzilli, *Inorg. Chem.*, 2005, **44**, 7644–7651.
63 V. Beljanski, J. M. Villanueva, P. W. Doetsch, G. Natile and L. G. Marzilli, *J. Am. Chem. Soc.*, 2005, **127**, 15833–15842.
64 K. M. Williams, L. Cerasino, G. Natile and L. G. Marzilli, *J. Am. Chem. Soc.*, 2000, **122**, 8021–8030.
65 R. Ranaldo, N. Margiotta, F. P. Intini, C. Pacifico and G. Natile, *Inorg. Chem.*, 2008, **47**, 2820–2830.
66 L. T. Ellis and T. W. Hambley, *Acta Crystallogr., Sect. C: Cryst. Struct. Commun.*, 1994, **50**, 1888–1889.
67 C. J. L. Lock and P. Pilon, *Acta Crystallogr., Sect. B: Struct. Crystallogr. Cryst. Chem.*, 1981, **37**, 45–49.
68 L. Kelland, *Nat. Rev. Cancer*, 2007, **7**, 573–584.
69 J. Kasparkova, T. Suchankova, A. Halamikova, L. Zerzankova, O. Vrana, N. Margiotta, G. Natile and V. Brabec, *Biochem. Pharmacol.*, 2010, **79**, 552–564.
70 N. Margiotta, C. Marzano, V. Gandin, D. Osella, M. Ravera, E. Gabano, J. A. Platts, E. Petruzzella, J. D. Hoeschele and G. Natile, *J. Med. Chem.*, 2012, **55**, 7182–7192.
71 V. Brabec, J. Malina, N. Margiotta, G. Natile and J. Kasparkova, *Chem. – Eur. J.*, 2012, **18**, 15439–15448.
72 N. Margiotta, R. Ranaldo, F. P. Intini and G. Natile, *Dalton Trans.*, 2011, **40**, 12877–12885.
73 E. Petruzzella, N. Margiotta, M. Ravera and G. Natile, *Inorg. Chem.*, 2013, **52**, 2393–2403.
74 G. Raudaschl, B. Lippert, J. D. Hoeschele, H. E. Howard-Lock, C. J. L. Lock and P. Pilon, *Inorg. Chim. Acta*, 1985, **106**, 141–149.
75 T. Ishibashi and S. J. Lippard, *Proc. Natl. Acad. Sci. U. S. A.*, 1998, **95**, 4219–4223.
76 J. M. Villanueva, X. Jia, P. G. Yohannes, P. W. Doetsch and L. G. Marzilli, *Inorg. Chem.*, 1999, **38**, 6069–6080.
77 T.-L. Hwang and A. J. Shaka, *J. Magn. Reson., Ser. A*, 1995, **112**, 275–279.
78 *CRC Handbook of Biochemistry and Molecular Biology*, CRC Press, Cleveland, OH, 3rd edn, 1975, vol. I.
79 J. D. Hoeschele, H. D. H. Showalter, A. J. Kraker, W. L. Elliott, B. J. Roberts and J. W. Kampf, *J. Med. Chem.*, 1994, **37**, 2630–2636.
80 T. P. Johnston, G. S. McCaleb, S. D. Clayton, J. L. Frye, C. A. Krauth and J. A. Montgomery, *J. Med. Chem.*, 1977, **20**, 279–290.
81 S. Shamsuddin, I. Takahashi, Z. H. Siddik and A. R. Khokhar, *J. Inorg. Biochem.*, 1996, **61**, 291–301.
82 J. J. P. Stewart, *MOPAC2009, Stewart Computational Chemistry*, Colorado Springs, CO, USA, 2008, http://OpenMOPAC.net.
83 J. J. P. Stewart, *J. Mol. Model*, 2007, **13**, 1173–1213.
84 M. Korth, M. Pitonák, J. Rezác and P. Hobza, *J. Chem. Theor. Comp.*, 2010, **6**, 344–352.
85 R. J. Deeth, A. Anastasi, C. Diedrich and K. Randell, *Coord. Chem. Rev.*, 2009, **253**, 795–816.
86 A. Anastasi and R. J. Deeth, *J. Chem. Theor. Comput.*, 2009, **5**, 2339–2352.
87 H.-C. Tai, R. Brodbeck, J. Kasparkova, N. J. Farrer, V. Brabec, P. J. Sadler and R. J. Deeth, *Inorg. Chem.*, 2012, **51**, 6830–6841.
88 J. Wang, P. Cieplak and P. A. Kollman, *J. Comput. Chem.*, 2000, **21**, 1049–1074.
89 R. J. Deeth, N. Fey and B. J. Williams-Hubbard, *J. Comput. Chem.*, 2005, **26**, 123–130.
90 MOE: Molecular Operating Environment, 2011.10; Chemical Computing Group: Montreal, 2011.
91 K. Wüthrich, *NMR of Proteins and Nucleic Acids*, John Wiley & Sons, New York, 1986.
92 W. Saenger, *Principles of Nucleic Acid Structure*, Springer-Verlag, New York, 1984.
93 D. Over, G. Bertho, M. A. Elizondo-Riojas and J. Kozelka, *J. Biol. Inorg. Chem.*, 2006, **11**, 139–152.
94 V. Maheshwari, P. A. Marzilli and L. G. Marzilli, *Inorg. Chem.*, 2011, **50**, 6626–6636.
95 J. Kaspárková, K. J. Mellish, Y. Qu, V. Brabec and N. Farrell, *Biochemistry*, 1996, **35**, 16705–16713.
96 D. J. Patel, S. A. Kozlowski, A. Nordheim and A. Rich, *Proc. Natl. Acad. Sci. U. S. A.*, 1982, **79**, 1413–1417.

